Concentration Effects in Aqueous NaCl Solutions. A Molecular Dynamics Simulation.

Alexander P.Lyubartsev*† and Aatto Laaksonen††

Division of Physical Chemistry,

Arrhenius Laboratory, Stockholm University,

106 91 Stockholm SWEDEN

† - e-mail: sasha@tom.fos.su.se

†† - e-mail: aatto@tom.fos.su.se

A series of constant-temperature/constant-pressure molecular dynamics simulations of aqueous NaCl solution at different salt concentrations is carried out to investigate the structure and the dynamical properties. The simulations were performed with the number of molecules ranging from 256 to 2000. The simulations cover several nanoseconds to ensure the convergence of the results and enabling a proper determination of ion-ion radial distribution functions. The flexible SPC water model is used as the solvent, while the ions are treated as charged Lennard-Jones particles. Only a weak influence of the salt concentration is found on the ion-ion pair correlation functions. The structures of the hydrated shells around ion pairs are studied using three-body correlation functions. The self-diffusion and interdiffusion coefficients are found decreasing with an increase of salt concentration. Molar conductivities are calculated at different salt concentrations. Residence times of water molecules in the hydration shells as well as residence times of contact and solvent-separated ion configurations are determined.

---

* also affiliated with Scientific Research Institute of Physics, St.Petersburg State University, 198904, St.Petersburg, Russia.

1. Introduction

Computer simulations of aqueous ionic solutions have received much attention due to their importance in many areas of physical chemistry and molecular biophysics[1,2]. Studies of the structure of the hydrated shells around the ions[3-7], calculations of the ion-water radial distribution functions[5-10], energetics and thermodynamics of ion-water interactions[11-14], calculations of the potential of mean force at infinite dilutions[4,15-20] have been reported in literature. Most of these studies are done by simulating a single ion or an ion pair in water solution.

Despite of their importance, ionic solutions at finite concentrations, *i.e.* when at least several ion pairs are present, are considerably less studied using computer simulations One of the key issues in studies of concentrated ionic solutions is the ion-ion correlation, which can be described using radial distribution functions (RDF). The interionic RDFs are related to the potential of mean force (PMF) of ions[19] and to the effective interaction potential of ions in solution[21]. A knowledge of realistic PMFs or effective ion-ion potentials becomes particularly important in simulation studies of large biomolecular and other polyelectrolyte systems, where an explicit account of solvent molecules is still too expensive and one has to use simplified models with an effective account of the solvent.

The reported RDF[21-24] or PMF[15-20] results appear to be quite often in contradiction to each other and show an apparent dependence on the used model. A general picture arises in several works: the anion-cation potential of mean force has usually two minima, first corresponding to the contact ion pairs (CIP configuration) and the second corresponding to the solvent separated ion pairs (SSIP configuration). However the intensities, *i.e.* the relative importances of these minima vary largely from work to work. For example, the first minimum of the NaCl PMF is reported between -2 kJ/M (ref.[17]) and -20 kJ/M (ref.[15]).

Correspondingly, the first maximum of the Na-Cl RDF varies considerably in different works[21-26]. These differences can be explained partially by the different models, used for water and the ions. Another problem is that the determination of the potential of mean force requires expensive free energy simulations. While in the calculations of the radial distribution functions, one faces with poor statistics because of the low ratio of the number of ions to the total number of molecules and the low (comparatevely to the typical simulation time) mobility of the ions. A final difficulty is the necessity of an accurate treatment of the long range electrostatic interactions[15] in systems where the Debye radius typically has the order of the box length.

Under these circumstances it is important to carry out an extended analysis of the existing ionic solution models and to try to take into account all possible sources of artifacts and weaknesses. It is necessary to investigate the effects of the limited simulation time, use of the finite cutoff radii in force calculations, evaluate the details and performance of the molecular dynamics algorithms, to mention a few. In this paper we present a rather extensive molecular dynamics study of aqueous NaCl solution. We have performed a series of sufficiently long (several nanoseconds) simulations at different salt concentrations, ranging from 0.5M to 4M. The molecular and potential models and details of molecular dynamical algorithm are described in Sec.2. In Sec.3 we present results on ion-ion radial distribution functions, including an analysis of statistical errors, as well as the effects of simulation time and the system size. We have also analyzed the structures of the hydrated shells around ions and ion pairs using three-body correlation functions.

In addition to the hydration structure and interionic correlations, the dynamical behaviour of the ions in solution and the waters hydrating the ions are of central importance. Molecular dynamics simulations can give a direct insight into the molecular motion, which can be helpful for understanding and interpretation of results obtained from NMR studies, conductivity

measurements, and other experimental techniques. For more information about the experimental work, the reader is referred to the review by Ohtaki and Radnai[2]. A variety of dynamical properties of ionic solutions have been studied using molecular dynamics simulations [27-30]. The information about the behavior of hydrated water molecules and the hydrated ions themselves is still rather limited and fragmented [2]. In Sec.4 we present results of time autocorrelation functions, self-diffusion and interdiffusion coefficients, residence times and their concentration dependences. Finally the conclusions are summarized in Sec. 5.

2. Models and Methods

There exist a large number of water and water-ions interaction models in literature, from simple dipole hard sphere[31] or Stockmayer liquid[32] to interaction potentials, obtained from *ab initio* quantum mechanical calculations[33] . The more realistic is the used potential model, the more computer time is required for the simulations. In this work we have used a standard type of force field, in which all the intermolecular interaction are expressed as a sum of the electrostatic and the Lennard-Jones potentials with parameters, fitted for each atomic type. This type of the force field is rather simple and allows to make the computions fast. Nevertheless, these potentials have shown to give a realistic description of intermolecular interactions provided that the interaction parameters are properly fitted. We have chosen the flexible SPC water model[34] and the Smith-Dang parameters for ion-water and ion-ion interactions[8,27]. The atom-atom potentials are expresssed as:

$$\psi\left(r_i, r_j\right) = \frac{q_i q_j}{r_{ij}} + 4\varepsilon_{ij}\left[\left(\frac{\sigma_{ij}}{r_{ij}}\right)^{12} - \left(\frac{\sigma_{ij}}{r_{ij}}\right)^{6}\right] \qquad (1)$$

where off-diagonal Lennard-Jones parameters σ_{ij} and ε_{ij} are given using the combination rules [35]:

$$\sigma_{ij} = \left(\sigma_i + \sigma_j\right)/2,$$
$$\varepsilon_{ij} = \sqrt{\varepsilon_i \varepsilon_j}$$

The potential parameters q_i, σ_i and ε_i are given in Table 1. The parameters for the ions are determined in ref.[8] by fitting them to a gas-phase binding enthalpy data for small sodium and chlorine ion-water clusters. This fitting was done for the SPC/E water model. In our work we used the flexible SPC model, which has almost the same parameters and structural properties as SPC/E model. The flexible SPC model contains some polarization effects due to its flexibility. The diffusion coefficient and the dielectric constant of the flexible SPC model are very close to the experimental values[36]. These features of this particular water model should be important for studies of ionic solution with strong electrostatic interactions.

We used constant-temperature constant-pressure molecular dynamics algorithm[37] in our MD simulations. The Nose-Hoover thermostat parameters were set to 30fs for the thermal bath and 700fs for the volume fluctuations. In all our simulations the temperature was 300K and the pressure was 1 atm. Other characteristic simulation parameters are given in Table 2. The simulations were performed at four different salt concentrations. In addition, two of these (0.55M and 0.9M) were made with different box sizes to evaluate possible size effects. A separate 200ps simulation was made for 256 water molecules without ions to have a reference data for the bulk water.

All the simulations were carried out in a cubic box with periodic boundary conditions, using minimum image convention. The Ewald method was applied

for treatment of long range electrostatic interactions[38]. The cutoff radius in the reciprocal space, k_{max}, was determined from the condition that the exponent factor in the k-space term, $exp(-\pi^2 k_{max}^2/(L\alpha)^2)=exp(-8.5)$, and the screening parameter α was taken as $\alpha=2.8/R_{cut}$. Under these conditions the cutoff distance in the real space R_{cut} can be optimized for a maximum computation speed (evidently, a decrease of R_{cut} reduces the computation time for the real space term while it increases the computation time for the reciprocal space term). In our largest simulation with 2000 molecules, we have used R_{cut}=14Å, while in other cases the cutoff distance was set equal to a half of the box length.

In the starting configuration, the molecules were located with random orientations on the FCC lattice, the ions being distributed randomly in the volume. Then the system was equilibrated during 200ps. We have used the double time step algorithm by Tuckerman et al. [39], with a small time step of 0.2 fs for intramolecular and short range (less than 4.5Å) intermolecular interactions, and a large time step of 2 fs for the other interactions. Our test simulation in the constant-energy ensemble clearly showed that larger time steps than 0.2/2.0 fs, led rapidly to a poor energy conservation and to a noticeble shift in the calculated pressure. The calculations were carried out on an IBM SP2 at the center of parallel computing (PDC), the Royal Institute of Technology, Stockholm.

3. Static Properties.

3.1. Thermodynamical properties.

The results for the density of NaCl solution at different concentrations are given in Table 3 together with the experimental densities of the NaCl solution. There is a small difference (0.01g/cm^3) between the experimental and the calculated densities which is constant throughout the concentration interval. This may be a consequence that the original flexible SPC model has somewhat higher

density compared to the experimental one. Our simulations of pure water shows that the density of the flexible SPC water is 1.006g/cm^3. This is in agreement with the NVT simulations by Wallqvist and Teleman [40] who found that at experimental density, this model gives a negative pressure.

The different contributions into total energy are also presented in the Table 3. One can see that water-water interaction energy E(H_2O-H_2O) is increasing (becomes less negative) with an increase of the salt concentration. This effect takes place mainly due to the disruption of the hydrogen bonds. The ion-water interactions, (E(Na+ -H2O) and E(Cl- - H_2O)) both become weaker upon the increase of the salt concentration, because of the influence of other ions on the hydrated shell. An interesting observation is that the total interaction energy of an ion with other molecules is less sensitive to the salt concentration. The increase of the ion-water energy becomes compensated by the decrease of the ion-ion energy. The same holds for water molecules (see the term "E(H_2O with others)" in Table 3), for which the weakening of the hydrogen bonds is compensated by a larger contribution from ion-water interactions.

The total solvation energy can be determined as the energy for the process of transfering the solute molecules from the ideal gas phase into the solvent, and it is equal to the difference of the total energy of the solution and energy of the same amount of the bulk water. These values are listed in Table 3. The solvation energy at infinite dilution is taken from ref.[27] which was calculated for a separated (more than 6Å) Na-Cl ion pair using the same ion model as in our work but a rigid SPC/E water model. One can see a non-monotonous dependence on the salt concentration, with a weak minimum at concentration about 1M. This means that it is energetically more profitable to install ion pairs in solution at this concentration. It is quite remarkable that the experimental dependence of NaCl activity coefficients[42] also shows a minimum at this concentration. The connection here is not direct: the activity coefficients are

related to the free energy and its concentration dependence. At the same time, the internal energy gives a major contribution to the free energy.

3.2. Structural pair correlations.

The structure of liquids and solutions can be conveniently studied using radial distribution functions. Calculations of radial distribution functions is usually a straightforward task in molecular dynamics simulations. The water/water and water-ion correlation functions, calculated in our simulations are in perfect agreement with corresponding results from other simulations[5-10]. The hydration numbers, obtained by integrating of the first minimum of ion-oxygen RDF, are presented in Table 3. It can be observed that the Na+ hydration number is steadily decreasing with the increase of the salt concentration. This is most likely because some water molecules in the hydration shell are occasionally substituted by chlorine ions. This effect does not take place for the chlorine hydration numbers. A sodium ion, forming a contact ion pair with a clorine ion, does not substitute a water molecule in the hydration shell around chlorine. It rather installs itself there. As a result of this, the size of the Cl- hydration shell increases slightly with the salt concentration.

Obtaining the ion-ion RDFs is a matter of much more efforts than calculations of the ion-water RDF. In fact, we have found that a reliable evaluation of the ion-ion RDFs requires a simulation time of several nanoseconds. The main reason for the extended simulations is the small number of ions in the simulation cell, resulting in a poor statistics. In addition, a slow ion diffusion leads to a slow sampling of the configurational space. Thus, the characteristic time which is required for a considerable change of ion configuration has the order of hundred picoseconds. In Table 4, we present some results, obtained from averaging over several sequential 500ps pieces of the simulations. The first observation is that the results for the first maximum of NaCl RDF are unstable, varying more than one order of magnitude. The reason

for this behaviour is that the CIP and SSIP configurations are separated by a high (several kT) effective potential barrier and transitions between them are rare events (detailed analysis of corresponding residence time will be given in the next section). The ion-water interaction energies also fluctuate strongly which leads to relatively high statistical errors for these energies. Moreover, some correlation between the water-ion interaction energies and the value of the first maximum of NaCl RDF can be seen from Table 4. A low value of this maximum corresponds to low values of ion-water energies. The ions in this case are almost fully hydrated and do not come into direct contact with each other. On the contrary, an occasional formation of contact ion pairs leads to weaker ion-water interactions.

The case with the lowest salt concentration, presented in Table 4, is worst from the statistical point. The other simulations contain more ion pairs, giving a better sampling statistics even after a shorter simulation time. Still we may consider a simulation time of the order of one nanosecond as a minimum requirement for a reliable evaluation of ion-ion RDF.

The resulting ion-ion RDFs are presented in Figures 1-3. The typical features of these RDFs correspond to the results obtained previously in other simulations[21-25] and to the potential of mean force calculations[15-19]. The NaCl RDF have a first contact maximum at 2.8Å, second solvent separated maximum at 5.1Å and a weak third maximum at about 7Å corresponding to an attraction of fully hydrated ions. The RDFs between the like-charged ions also have several maxima. The RDFs show a rather weak dependence on salt concentration. The most noticeable effects of the increase of the salt concentration are an increase of the first maximum and decrease of the second and third maxima of the NaCl RDF. The RDFs for like-charged ions tend to increase with increasing of salt concentration.

Having obtained the ion-ion RDFs, we can determine how many ions occur in the contact or in the solvent separated configurations. This can be done

by integrating the corresponding maximum of ion-ion RDF in the same way as one calculates the hydration numbers:

$$x = c\int_{r_1}^{r_2}\rho(r)4\pi r^2 dr \qquad (2)$$

Relative populations of CIP and SSIP states are important quantities in the theory of ionic association [43] and can be measured using infrared and Raman spectroscopy [44]. The values calculated in our work, are listed in Table 3. One can see that in 0.5 M solution only about 4% of ions form ion pairs, whereas at 4M concentration about a half of the ions are in contact with opposite ions.

Differences in RDFs, obtained at the same concentration but varying the system size, are generally small. One can note that the second maximum of the NaCl RDF is higher for larger systems, however the difference is of the same order as the statistical error. Also, some differences are observed at large distances close to the half box length, which most likely take place due to boundary effects.

3.3 Three-body correlation functions.

The radial distribution functions do not give a full description of the structural properties. In general, an average spatial assembly of more than two particles cannot be uniquely characterized from pair correlation functions. Additional information can be obtained from three- and higher-order correlation functions.

Calculations of higher-order correlation functions is a straithforward task in computer simulations, they are calculated in the same manner as the RDFs. The three-body distribution function $\rho_3(r_1,r_2,r_3)$ for a spacially and orientationally homogenious system is a function of three variables. For example, the three distances between the three particles. It is, however, rather difficult to display this function of three variables in a two-dimensional figure. To simplify the task, one may fix one of the variables, say, the distance between

the first and the second particle r_{12}, and build a contour map of the function of the two remaining variables. This function is proportional to the density distribution of the third particle in the vicinity of fixed first and second particles:

$$\rho(r_3|r_{12}=\text{const}) = \rho_3(r_1,r_2,r_3)/\rho_2(r_{12})$$

where $\rho_2(r_{12})$ is the RDF between the 1:st and the 2:nd particle. The distance r_{12} can be taken corresponding to a maximum of RDF between these two particles. In this case the maxima of the $\rho(r_3|r_{12}=\text{const})$ function show typical configurations for the three particles. In three-dimensional space this function has an axial symmetry with respect to the line connecting the first and the second particle.

Examples of three-body distribution functions are shown in Fig.4-7 [45]. They were taken from the run 4, corresponding to 0.9M concentration. In Fig.4, contour maps of oxygen distribution (solid lines) and hydrogen distribution (dashed lines) around Na and O atoms separated on 2.35Å are displayed. Positions of oxygen atoms in the first hydration shell are well defined, they are located in three perpendicular directions from sodium ion and yield hydration number 6. The second hydration shell shows clearly an octahedral shape.

The structure of clorine hydration shell (oxygen and hydrogen distributions around Cl-O pair) is shown in Fig.5. There is no such well-defined symmetry as can be seen in the case of the sodium ion. Positions of the two water molecules in the hydration shell are hardly correlated, with the exception that they cannot come too close to each other. There are no noticeable second hydration shell around clorine ion.

The structure of the hydration shell around the contact ion pair is shown in Fig. 6. It can be seen that the hydration shell of the ion pair repeats typical features of pure sodium and clorine shells (Fig.4,5). It looks like one of the ions

is entering into the hydration shell of the other ion instead of one of the water molecules. It does not seem to change the rest of the hydration shell noticably.

The distributions of oxygen and hydrogen around the solvent-separated ion pair are shown in Fig.7. The positions and the orientations of the water molecule linking the two ions are well defined. This water molecule is not found on the line between the sodium and the clorine ions. It seems to rather orient itself with respect to the each of the ions in the same fashion as was found in the hydration shell of an isolated ion (compare Figures 4 and 5). The positions of other oxygens in the sodium hydration shell are somewhat diffuse with respect to the clorine ion.

4. Dynamical properties.

4.1. Velocity autocorrelation functions

The normalized velocity autocorrelation function (VACF) is defined as

$$f_v(t) = \frac{\left\langle v_i(t_0 + t) v_i(t_0) \right\rangle_{i,t_0}}{\left\langle v_i(t_0)^2 \right\rangle_{i,t_0}} \qquad (3)$$

- where the averaging is taken over both particle number i and time t_0. The calculated VACF for the water molecules and the ions at different salt concentrations are shown in Figures 8-10. VACFs appear to have a rather weak dependence on salt concentration. An increase of salt concentration leads to some strengthening of the negative part of VACF, most noticeable on the time scale of 0.1 - 0.3 ps. This means a greater probability for a particle to turn back after this time, and hence an enhancement of the oscillations in the microscopic dynamics of the molecules and slowing down of the diffusion.

Analoguously with eq. (3), the normalized angular velocity auto-correlation functions can be defined as:

$$f_w(t) = \frac{\langle w_i(t_0 + t) w_i(t_0) \rangle_{i,t_0}}{\langle w_i(t_0)^2 \rangle_{i,t_0}} \qquad (4)$$

The angular VACF for water molecules is also displayed in Fig.8. It decays much faster than the translational VACF. No noticeable dependence of $f_w(t)$ on salt concentration was found.

4.2 Self-diffusion.

The translational self-diffusion coefficients can be determined by two methods :

- from mean square displacement

$$D = lim_{t->\infty} \frac{\langle [R(t) - R(0)]^2 \rangle}{6t} \qquad (5)$$

- or from the velocity autocorrelation functions:

$$D = \frac{kT}{m} \int_0^\infty f_v(t) dt \qquad (6)$$

We have used both methods to determine D. While calculating the diffusion coefficients from mean square displacement we have taken the slope of the curve in eq. (5) at time t between 50 and 200ps. In fact, the convergence within 5% interval was already reached after about 10 ps. Attempts to calculate the mean square displacement on a longer time scale lead to a growing uncertainty due to a worsening of sampling statistics when time t becomes comparative with the simulation time. The mean square displacements of ions are displayed in Fig.11. One can see that during 0.5ns the ions in average travel on distance 10-15Å which is less then the box size and comparative (especially for low salt concentrations) with the average distance between the ions. This is

the main reason why we need so long time to calculate ion-ion distribution functions.

The final results for the self-diffusion coefficients are presented in Table 5. All the diffusion coefficients, both for water and for ions, decrease with increasing of salt concentration as expected, an especially noticable fall of the diffusion coefficients takes place at high salt concentrations. There exists other simulation data of self-diffusion coefficients of ions, calculated at infinite dilution (a single ion in the cell). Lee and Rasaiah[41] obtained for the same model of ions and SPC/E water $D_{Na+}=1.2\cdot10^{-5}cm^2/s$ and $D_{Cl}=1.7\cdot10^{-5}cm^2/s$. Guardia *et al* [17] obtained for Pettitt-Rossky ion model and flexible SPC water $D_{Na+}=1.1\cdot10^{-5}cm^2/s$ and $D_{Cl-}=2.5\cdot10^{-5}cm^2/s$. Simulations of Na+ ion in TIP4P water yield sufficiently lower diffusion coefficient: $D_{Na+}=0.74\cdot10^{-5}cm^2/s$ in ref.[29] and $D_{Na+}=0.67\cdot10^{-5}cm^2/s$ in ref.[46]. For Cl- ion in TIP4P water self-diffusion coefficient was obtained in ref.[28] as $D_{Cl-}=1.57\cdot10^{-5}cm^2/s$. It has been observed also that the way to treat the long-range electrostatic forces strongly affects the calculated diffusion coefficients [28,40].

The self-diffusion coefficient for bulk water was obtained as $D_v=2.2\cdot10^{-5}$ cm^2/s (run 0). This result is lower then previous estimations for the flexible SPC model ($D_v=2.54\cdot10^{-5}cm^2/s$ in ref.[36] and $D_v=3.1\cdot10^{-5}$ cm^2/s in ref.[40]) but it is closer to the experimental diffusion coefficient of water $2.35\cdot10^{-5}cm^2/s$ [42]. As well as our results, experimental data [47] also shows an decrease of diffusion coefficient of water with increasing of salt concentration, although this effect is more pronounced in our simulation.

4.3. Interdiffusion.

Interdiffusion coefficient D_{12} is determined from the time integration of normalized current correlation function J(t) [48]:

$$D_{12} = kT\frac{m_1 + m_2}{2m_1m_2}\int_0^\infty J(t)dt \qquad (7)$$

$$J(t) = \frac{\langle j(t)j(0)\rangle}{\langle |j(0)|^2 \rangle} \qquad (8)$$

- where:

$$j(t) = \sum_{i=1}^{N} q_i v_i(t) \qquad (9)$$

is a microscopic estimator of the current flow. If the ions move independently from each other, the interdiffusion coefficient is equal to the mean value of their self-diffusion coefficients. Ion-ion association and correlations in the ion motion lead to a deviation between the interdiffusion coefficient and the mean self-diffusion coefficient, which is described by a parameter Δ [30]:

$$D_{12}=(1-\Delta)(D_1+D_2)/2 \qquad (10)$$

The interdiffusion coefficient is also related to the equivalent (or molar) conductivity of ionic solution:

$$\Lambda = \frac{2N_A e^2}{kT} D_{12}$$

Calculated values of interdiffusion coefficients and equivalent conductivities, together with the corresponding experimental values, are given in Table 6. The calculated conductivities are systematically somewhat less than the experimental ones[49]. This is a consequence of the overall slower diffusion in the chosen potential model comparing with the experimental data (see Table 5). Still, the calculated and experimental conductivities have the same trend and the difference between them is nearly constant throughout the concentration range.

The interdiffusion coefficients are somewhat lower than average of self-diffusion coefficients. This is a consequence of ionic association. Opposite charged ions in an ion pair tend to move together making a negative contribution from non-diagonal terms in eq.(8) into the current correlation function. This effect more or less disappears at very high concentrations (Δ=0.02 for 4M solution), because most of the ions have several (accounting solvent-separated) neighbours and no isolated ion pairs exist.

To observe directly correlations in the motion of ions, we calculated the following function. Let two ions occur on distance R_0 at moment t = 0 with their coordinates $r_1(0)$ and $r_2(0)$. We will follow their motion and calculate the scalar product of their displacements, averaging over all such pairs:

$$\rho(R_0, t) = \left\langle (r_1(t) - r_1(0))(r_2(t) - r_2(0)) \right\rangle \Big|_{|r_1(0) - r_2(0)| = R_0} \qquad (11)$$

If two ions form a stable ion pair and move together, this function would be proportional to time t (as mean square displacement of a single particle). If motion of the ions is by no means correlated (for example, at very large R_0), this function is equal to zero. In other cases we can expect an intermediate behavior.

We have calculated function $\rho(R_0,t)$ for (Na^+ , Cl^-) pairs at two values of R_0 corresponding to a contact (R_0=2.81Å) and to a solvent separated (R_0=5.1Å) ion pairs. The results are shown in Figures 12 and 13. For a contact ion pair at 0.5M concentration the slope of the function $\rho(R_0,t)$ is almost the same as for the self-diffusion of Na^+ ion (fig. 4). For higher concentrations, the correlations become weaker in ion motion. These are also several times weaker for solvent-separated ion pairs (see fig.10) and almost disappear for ions separated more than 7Å from each other.

4.4. Residence time.

How long water molecules stay in the hydration shell around different ions at different physical conditions is important for understanding the dynamics of the hydrated water molecules[2]. For example, it is related to the "dynamic hydration number", which provides an estimate of the number of water molecules which are bound to an ion on a time scale in which the coordinated shell of a bulk water molecule is renewed [33].

We define a border of the hydration shell r_{hyd} as the first minimum of ion-oxygen RDF. Then, according to ref.[33], we define a function $P_j(t,t_i;t^*)$, which takes the value 1 if molecule j lies within the first coordination shell of the ion at both time steps t_i and t_i+t and in the interim does not leave the coordinated shell for any continuous period, longer than t^*. Otherwise it takes value 0. The parameter t* is introduced to ignore cases when a molecule leaves the coordinated shell only temporarily and returns back without properly entering the bulk solution. As in the other works [27,33] we set t^*=2ps.

Then we define a function:

$$p(t)=\langle P_j(t,t_i;t^*)\rangle_{i,j}/\langle P_j(0,t_i;t^*)\rangle_{i,j} \qquad (12)$$

which gives a probability for a molecule in the hydrated shell to remain there during time t. These functions are shown in Fig.14. After a fast initial fall they decays almost exponentially: $p(t)\sim\exp(-t/t_s)$ where t_s is the residence time.

The results obtained for the residence time at different concentrations are listed in Table 7. An interesting observation is that while the residence time for Cl^- increases with the increase of the salt concentration, it preserves generally the same value for Na+. The increase of the residence time for Cl^- ions may take place due to contribution from the ion pairs in which Cl^- and Na^+ ions share some of the water molecules with longer residence time.

A residence time for two water molecules, found in contact, is also increasing with the increasing salt concentration. This may be because more and more water molecules become involved in hydration of the ions and this will increase the average residence time for the waters. The residence times of water molecules in the hydration shells of ions are estimated in other works at an infinite dilution. Result of ref.[41] is 26ps for Na+ and 9.0ps for Cl- and result of ref.[27] is 29ps for Na+ and 12ps for Cl-. These results were obtained for the SPC/E water model and are similar to our results. For the MCY water model Impey *et al* [33] obtained much lower results: 10ps for Na+ and 4.5ps for Cl-.

In analogue to the residence time of water molecules, we can define a residence time of contact and solvent separated configurations of the ions. Because of a poor statistics of these events, we could not draw function p(t) properly to determine the decay parameter. Instead, we have used an averaging of time intervals during which the ions were in CIP or SSIP configurations, respectively. Observe that for a purely exponential decay, these two definitions are equivalent. The results are shown in Table 7. The residence time both for CIP and SSIP configurations does not seem to depend on the salt concentration, at least in the limits of statistical error. Contact configurations are more stable than solvent-separated. Average time for CIP configurations is about 50ps, but we have registered several cases when an NaCl contact pair existed a longer time than 200ps. The long-living CIP configurations were one of the obstacles for reliable RDF calculations, especially when only a few ion pairs are present in the simulation box (runs 1 and 3 in Table 1 for example). While a CIP configuration exists, it gives a strong contribution to the first maximum of the ion-ion RDF. Therafter a long period may follow, up to several hundred pico seconds, without any CIP configurations at all. This may also cause some unstability in the calculations of other properties.

5. Conclusions

We have carried out a series of molecular dynamics simulations of a model NaCl ionic solution at different concentrations and also varying the system size. The great benefit of computer simulations is the possibility to directly observe every molecular detail of the model system. Of course, the obtained information is relevant only in the extent how the interaction potentials are able to mimic the real system. The potentials employed in this work were derived mostly empirically by fitting to some experimental thermodynamical and structural data [8] and results preveously reported on this model were in line with other theoretical and experimental studies of NaCl ionic solutions.

An advantage of carrying out a series of simulations varying a parameter (e.g. concentration) is that such studies reveals some dependences and trends which are usually much less sensitive to the model in use than some specific quantities. Our studies of structural and dynamical aspects of the hydrated shell of ions, ion association vs salt concentration may contribute to deeper understanding of microscopic processes in solutions.

We have also checked a possible influence of the system size on the simulation results. Simulations, carried out for different system sizes but at the same ion concentrations yielded in mostly the same results and existing deviations were in the limits of statistical error. This may be considered as a confirmation that long range electrostatic interactions were properly taken into account using the Ewald method.

Acknowledgments.

This work was supported by the Swedish Natural Science Foundation (NFR) and by the Wenner-Gren Foundation. We are thankful to the Center for Parallel Computing (PDC) at the Royal Institute of Technology for granting the computer facilities.

References and Notes

(1) Heinzinger,K. *Physica*, **1985**, *131B*, 196.

(2) Ohtaki, H.; Radnai,T. *Chem.Rev.*, *1993*, *93*, 1157.

(3) Bounds,D.G. *Mol.Phys.*,**1985**, *54*,1335.

(4) Pettitt, B.M.; Rossky,P.J. *J.Chem.Phys.*,**1986**, *84*,5836.

(5) Belch, A.C.; Berkowitz,M.; McCammon, J.A. *J.Am.Chem.Soc.*, **1986**, *108*, 1755.

(6) Degreve,L.; Quintale Jr.,C. *Chem.Phys.Lett.*, **1993**, *208*, 530.

(7) Parera.L.; Berkowitz,M.L. *J.Chem.Phys.*,**1994**, *100*,3085.

(8) Dang,L.X.; Smith,D.E. *J.Chem.Phys.*, **1993**, *99*,6950.

(9) Hummer,G., Soumpasis,D.M. Neumann,N. *Mol.Phys.*, **1992**, *77*, 769.

(10) Migliore,M.; Forlini,S.L.; Spohr,E.; Palinkas,G.; Heinzinger,K. *Z.Naturforsch.*, **1986**, *41*, 826.

(11) Chandrasekhar,J.; Spellmeyer,D.C.; Jorgensen, W.L. *J.Am.Chem. Soc.*, **1984**, *106*, 903.

(12) Lybrand,T.P.; Chosh,I.; McCammon, J.A. *J.Am.Chem.Soc.*, **1985**, *107*, 7793.

(13) Jayaram,B.; Beveridge,D.L. *J.Phys.Chem.*, **1990**, *94*,7288.

(14) Gowda,B.T.; Benson,S.W. *J.Chem.Phys.*, **1983**, *79*,1235.

(15) Smith, D.E.; Haymet,A.D.J. *Fluid Phase Equilibria*, **1993**, *88*, 79.

(16) Dang,L.X.; Pettitt,B.M.; Rossky,P.J. *J.Chem.Phys*, **1992**, *96*, 4046.

(17) Guardia,E.; Rey,R.; Padro,J.A. *J.Chem.Phys.*, **1991**,*95*, 2823.

(18) Friedman,R.A.; Mezei,M. *J.Chem.Phys.*, **1995**, *102*,419.

(19) Pratt,L.R.; Hummer,G.; Garcia,A.E. *Biophys.Chem.*, **1994**, *51*, 147.

(20) Karim,O.A.; McCammon,J.A. *J.Am.Chem.Soc.*, **1986**, *108*, 1762.

(21) Lyubartsev,A.P.; Laaksonen,A. *Phys.Rev.E*, **1995**, *52*, 3730.

(22) Hummer,G.; Soumpasis,D.M.; Neumann, M. *J.Phys.: Condens. Matter*, **1994**, *6*, A141.

(23) Hummer,G.; Soumpasis,D.M.; Neumann,M. *Mol.Phys.,* **1993**, *81*, 1155.

(24) Zhu,S.B.; Robinson,G.W. *J.Chem.Phys.*, **1992**, *97*, 4336.

(25) Chialvo,A.A.; Cummings,P.T.; Cochran,H.D.; Simonson, J.M.; Mesmer,R.E. *J.Chem.Phys.*, **1995**, *103*, 9379.

(26) Llano-Restrepo,M., Chapman,W.G. *J.Chem.Phys.*, **1994**, *100,* 8321.

(27) Smith,D.E.; Dang,L.X. *J.Chem.Phys*, **1994**, *100*, 3757.

(28) Perera,L.; Essmann,U.; Berkowitz,M.L. *J.Chem.Phys.*, **1995**, *102*, 450.

(29) Lee,S.H., Rasaiah,J.C. *J.Chem.Phys*., **1994**, *101*, 6964.

(30) Payne,V.A.; Forsyth,M.; Ratner,M.A.; Shriver, D.F.; de Leeuw,S.W. *J.Chem.Phys.*, **1994**, *100*, 5201.

(31) Patey,G.N.; Valleau,J.P. *J.Chem.Phys.*, **1975**, *63*, 2334.

(32) Patey,G.N.; Carnie,S.L. *J.Chem.Phys.*, **1983**, *78*, 5183.

(33) Impey,R.W.; Madden,P.A.; McDonald,I.R. *J.Chem.Phys.*, **1983**, *87*,5071.

(34) Toukan,K.; Rahman,A. *Phys.Rev.B*, **1985**, *31*,2643.

(35) Hansen,J.P.; McDonald,I.R. "*Theory of Simple Liquids*", Acad.Press, London, 1976

(36) Anderson,J.; Ullo,J.J.; Yip,S. *J.Chem.Phys*, **1987**, *87*, 1726.

(37) Melchionna,S.; Coccotti,G.; Holian,B.L. *Mol.Phys.*, **1993**, *78*, 533.

(38) Allen,M.P.; Tildesley, D.J. "*Computer Simulation of Liquids"* , Clarendon Press, Oxford, 1987.

(39) Tuckerman,M.; Berne,B.J.; Martyna,G.J. *J.Chem.Phys.*, **1992**, *97*, 1990.

(40) Wallqvist,A.; Teleman,O. *Mol.Phys*., **1991**, *74*, 515.

(41) Lee, S.H.; Rasaiah,J.C. *J.Phys.Chem.*,**1996**, *100*,1420.

(42) CRC Handbook of Chemistry and Physics, Ed.D.R.Lide, CRC Press, 1994.

(43) S.Winstein, E.Clippinger, A.H.Fainberg and G.C.Robinson, *J.Am.Chem.Soc*., **1954**, *76*, 2597.

(44) "*Advances in Infrared and Raman Spectroscopy*", ed. R.J.Clark and R.E.Hester, Heyden, London, 1976.

(45) Color density maps of these and some other three-body correlation functions are available on author's WWW site:
http://www.fos.su.se/physical/sasha/shells/hydro.html

(46) Berkowitz,M.; Wan,W. *J.Chem.Phys*., **1987**, *86*, 376.

(47) Muller,K.J.; Hertz,H.G. *J.Phys.Chem*., **1996,** *100*, 1256.

(48) J.P.Hansen,J.P.; F.Joly,F.; and I.R.McDonald,I.R. *Physica A*, **1985**, *132*, 472.

(49) "*Lange's Handbook of Chemistry*", ed. J.A.Dean, McGraw-Hill, New York, 1985.

Table 1. Potential parameters.

Atom	q_i	σ_i(Å)	ε_i(kJ/M)
O	-0.82	3.1656	0.65
H	0.41	0.	0.
Na+	1.	2.35	0.544
Cl-	-1.	4.4	0.419

Table 2. Simulation parameters

Run No.	0	1	2	3	4	5	6
Number of H2O	256	490	1960	248	484	236	220
Number of ion pairs	0	5	20	4	8	10	18
Salt concentration (M)	0	0.55	0.55	0.87	0.9	2.2	4.1
Average box length (Å)	19.75	24.5	38.7	19.76	24.4	19.44	19.35
Simulation time (ns)[1]	0.2	2.5	1.5	3.5	2.	3.	3.

[1] - after 200 ps of equilibration

Table 3. Some thermodynamical and structural properties of aqueous NaCl solution. All the energies are given in kJ/M. For more details, see the text.

Run No.	0	1	2	3	4	5	6	statistical error
Salt concentration (M)	0	0.55	0.55	0.87	0.9	2.2	4.1	
Density, calculated (g/cm^3)	1.006	1.028	1.029	1.043	1.044	1.085	1.151	0.002
experimental[36]	0.997	1.02	1.02	1.033	1.034	1.076	1.14	
E_{tot}/N_{tot}	-41.9	-49.1	-49.2	-53.4	-53.7	-69.0	-91.3	0.1
Different contributions to the total energy:								
$E(H_2O\text{-}H_2O)/N_{H_2O}$[1]	-41.9	-35.9	-36.1	-33.1	-32.6	-25.5	-13.4	0.2
$E(Na+ - H_2O)/N_{Na}$	-745[2]	-675	-670	-590	-568	-443	-375	10
$E(Cl- - H_2O)/N_{Cl}$	-575[2]	-564	-561	-518	-505	-387	-340	15
$E(ion\text{-}ion)/N_{Na}$	-	-155	-163	-205	-223	-348	-404	15
E(H2O with others)[3]	-97.8	-98	-99.5	-100	-99	-99.5	-101	1
E(Na+ with others)[3]	-	-778	-780	-778	-785	-772	-773	10
E(Cl- with others)[3]	-	-725	-730	- 738	-752	-745	-755	15
$E_{solv.}/N_{ion\ pairs}$	-775 [4]	-807	-813	-820	-824	-802	-790	10
coordination numbers:								
Na+		5.78	5.8	5.5	5.6	5.42	5.3	0.05
Cl-		6.9	6.9	6.8	6.8	6.9	7.1	0.05
NaCl CIP configuration per ion		0.044	0.041	0.09	0.096	0.30	0.49	
NaCl SSIP configuration per ion		0.37	0.42	0.52	0.57	1.2	2.2	
NaNa SSIP configuration per ion		0.06	0.07	0.14	0.12	0.4	0.63	
ClCl SSIP configuration per ion		0.18	0.16	0.22	0.25	0.8	1.7	

[1] - including the intramolecular bond energy

[2] - result of ref.[41] for a single ion in SPC/E water

[3] - interaction energy of a selected molecule with all the other molecules

[4] - result of ref.[27] for a separated ion pair, the same ion model. and SPC/E water model.

Table 4. Some results of the simulation run No. 3, obtained from averaging over 0.5ns intervals of the MD trajectory.

averaging time (ns)	0.2-0.7	0.7-1.2	1.2-1.7	1.7-2.2	2.2-2.7	2.7-3.2	3.2-3.7	average	stat.error[1]
1-st max. NaCl RDF	8.2	4.8	3.2	0.6	3.	8.9	6.2	5.0	1.1
2-nd max. NaCl RDF	2.0	2.6	3.5	2.3	2.2	1.6	2.5	2.4	0.2
1-st max NaNa RDF	2.8	1.2	2.6	1.0	0.2	0.7	1.3	1.4	0.4
1-st max. ClCl RDF	1.2	1.1	0.6	1.5	1.3	1.7	0.7	1.15	0.15
$E(Na_+ - H_2O)/N_{Na}$(kJ/M)	-615	-548	-623	-625	-613	-568	-552	-592	11
$E(Cl- - H_2O)/N_{Cl}$ (kJ/M)	-434	-468	-522	-578	-543	-529	-523	-514	17

[1] - calculated as the corresponding variance, divided by $N^{1/2}$

Table 5. Diffusion coefficients (in 10^5 cm^2/s)

Run No.	exp[1]	0	1	2	3	4	5	6
Salt concentration (M)	0	0	0.55	0.55	0.87	0.9	2.2	4.1
a)Calculated from velocity autocorrelation functions								
H_2O	2.35	2.25	2.05	2.09	1.75	1.72	1.54	1.05
Na+	1.33	-	0.95	0.97	0.76	0.69	0.62	0.43
Cl-	2.03	-	1.24	1.28	1.03	1.06	0.89	0.53
b) Calculated from mean square displacements								
H_2O		2.12	2.01	-	-	1.66	1.49	0.97
Na+		-	0.88	-	0.69	0.70	0.63	0.42
Cl-		-	1.28	-	1.04	0.98	0.89	0.55
H_2O,experiment [47]	2.35				2.17		2.0	1.7

[1] - experimental results for infinite dilution [42]

Table 6. Interdiffusion coefficients D_{12} and molar conductivities Λ.

Concentration (M)	0.55	0.9	2.2	4.1
D_{12} ($10^5 cm^2/s$)	1.10	0.84	0.67	0.47
Δ[1]	0.03	0.05	0.08	0.02
Λ_{calc}($10^{-4} m^2 S\ mol^{-1}$)	83	63	52	38
Λ_{exp}(ref.[49])[2]	92	76	63	49

[1] - mean values of selfdiffusion coefficients calculated from VACF were used

[2] - at T=291K

Table 7. Residence times (in ps).

Concentration (M)	0.55	0.9	2.2	4.1	stat.error
H_2O-H_2O	4.7	4.9	5.4	6.5	0.1
H_2O-Na	21	20.5	22	22	0.5
H_2O-Cl	10.4	11	11.7	13.	0.5
NaCl , CIP	40±15	50±5	46	44	2
NaCl , SSIP	18	20	19.5	21	1

Captions.

Fig.1. Na-Na radial distribution functions.

Fig.2. Na-Cl radial distribution functions.

Fig.3. Cl-Cl radial distribution functions.

Fig.4. Contour map of oxygen (solid lines) and hydrogen (dashed lines) densities around Na+ and O atoms fixed at 2.35Å.

Fig.5. Contour map of oxygen (solid lines) and hydrogen (dashed lines) densities around Cl- and O atoms fixed at 3.21Å.

Fig.6. Contour map of oxygen (solid lines) and hydrogen (dashed lines) densities around Na+ and Cl- ions fixed at 2.81Å.

Fig.7. Contour map of oxygen (solid lines) and hydrogen (dashed lines) densities around Na+ and Cl- ions fixed at 5.1Å.

Fig.8. Translational and angular velocity autocorrelation functions of water molecules in the ionic solution.

Fig.9. Velocity autocorellation functions of Na+ ion at different concentrations.

Fig.10. Velocity autocorellation functions of Cl- ion at different concentrations.

Fig.11. Average displacement of an ion at different salt concentrations.

Fig.12. Displacement correlation function $\rho(R_0,t)$ for Na+Cl- contact pair (R_0=2.81Å, see eq.(11)).

Fig.13. Displacement correlation function $\rho(R_0,t)$ for Na+Cl- solvent separated pair (R_0=5.1Å, see eq.(11)).

Fig.14. Probability p(t) (see eq.(12)) for a water molecule in the coordinated shell of an ion to stay there after time t.

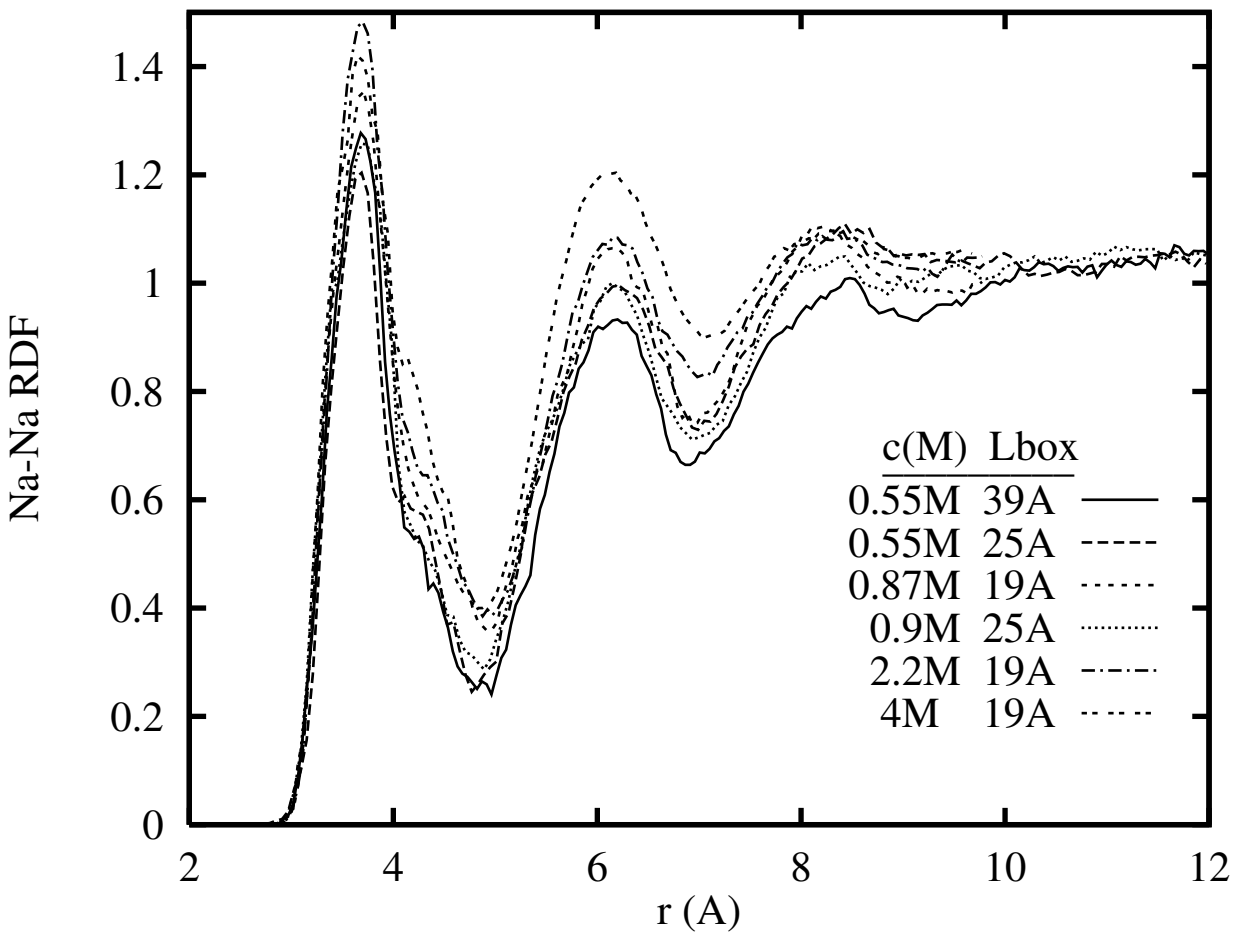
Na-Na RDF
r (A)
0
0.2
0.4
0.6
0.8
1
1.2
1.4
2
4
6
8
10
12
c(M) Lbox
0.55M 39A
0.55M 25A
0.87M 19A
0.9M 25A
2.2M 19A
4M 19A

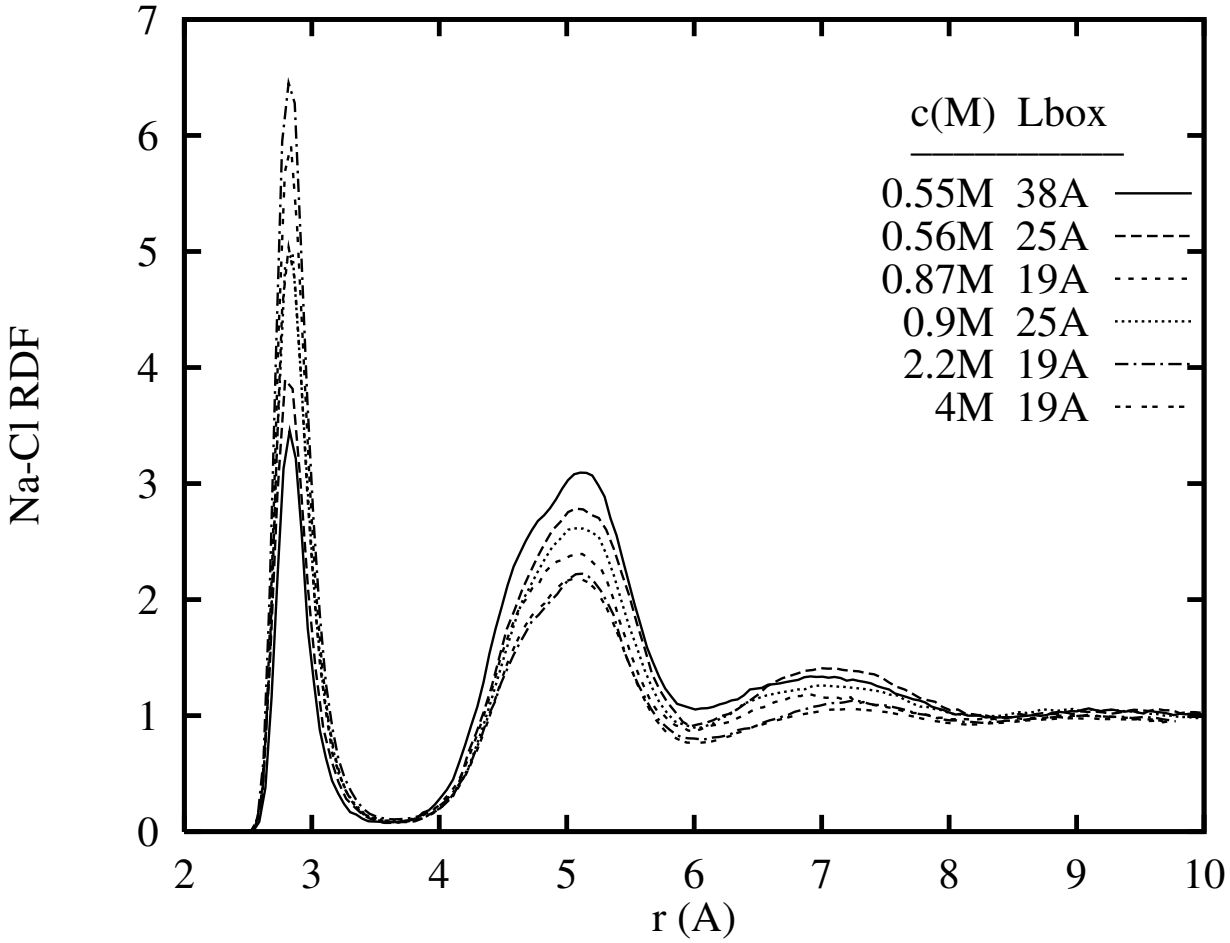
Na-Cl RDF
r (A)
c(M) Lbox
0.55M 38A
0.56M 25A
0.87M 19A
0.9M 25A
2.2M 19A
4M 19A
0
1
2
3
4
5
6
7
2
3
4
5
6
7
8
9
10

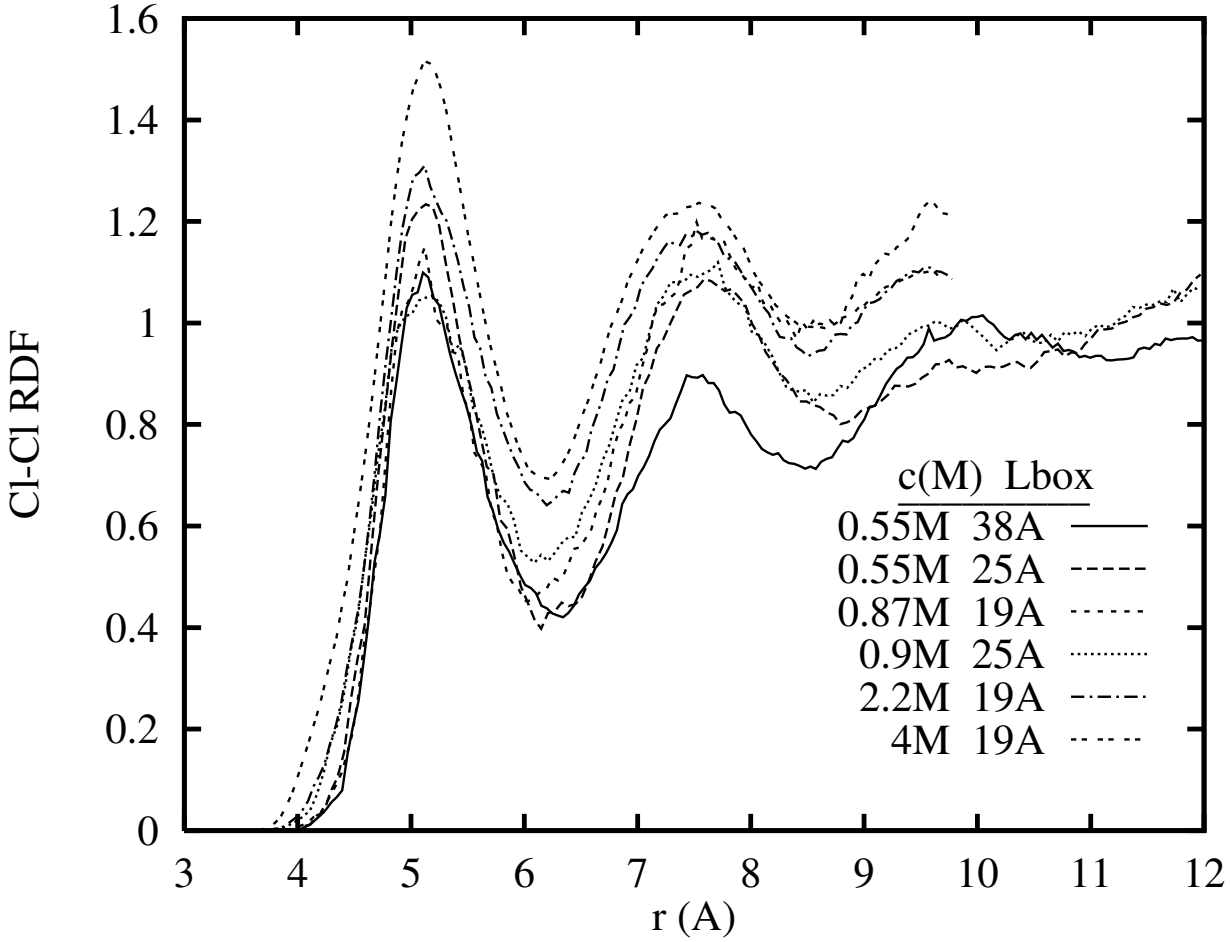
Cl-Cl RDF
r (A)
c(M) Lbox
0.55M 38A
0.55M 25A
0.87M 19A
0.9M 25A
2.2M 19A
4M 19A
0
0.2
0.4
0.6
0.8
1
1.2
1.4
1.6
3
4
5
6
7
8
9
10
11
12

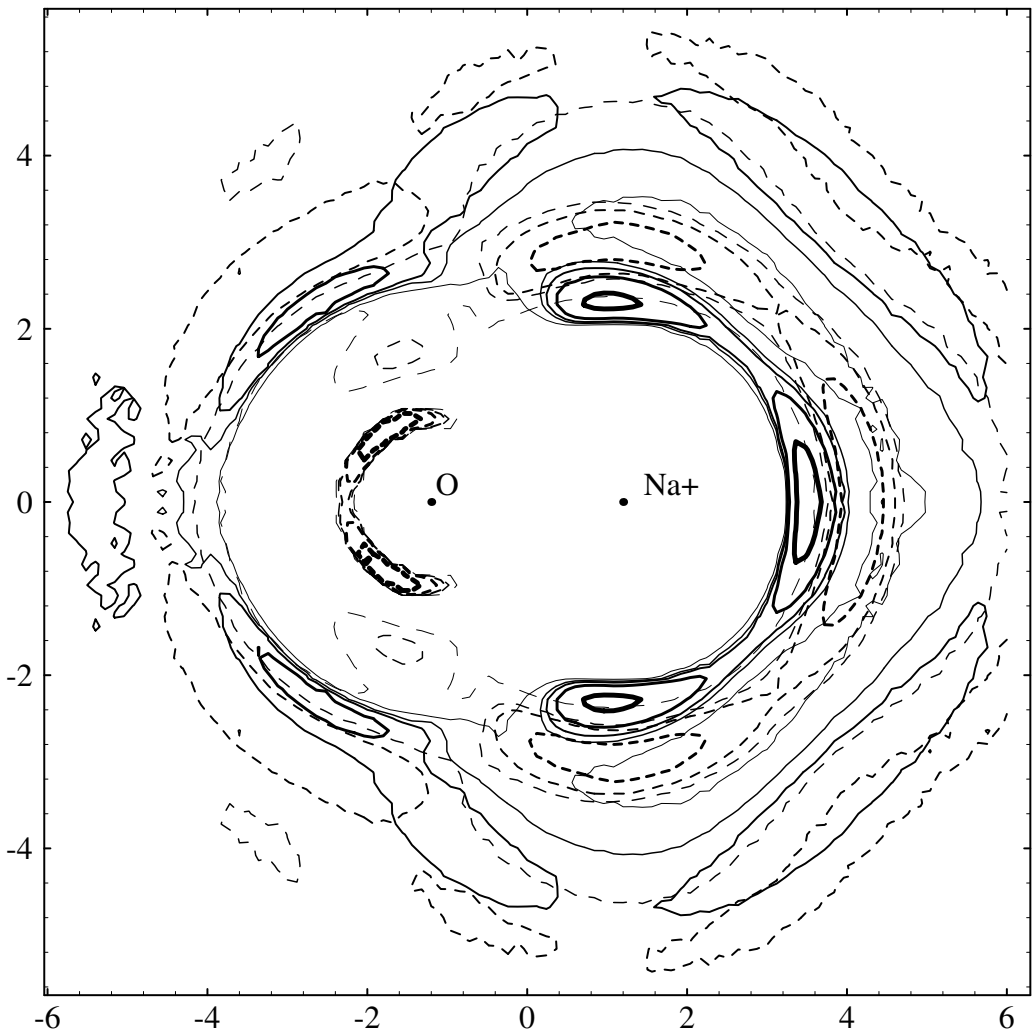

Intencities

O		H
———	0.2	– – – –
———	0.75	– – – – –
———	1.25	------
———	3	--------
———	15	----------

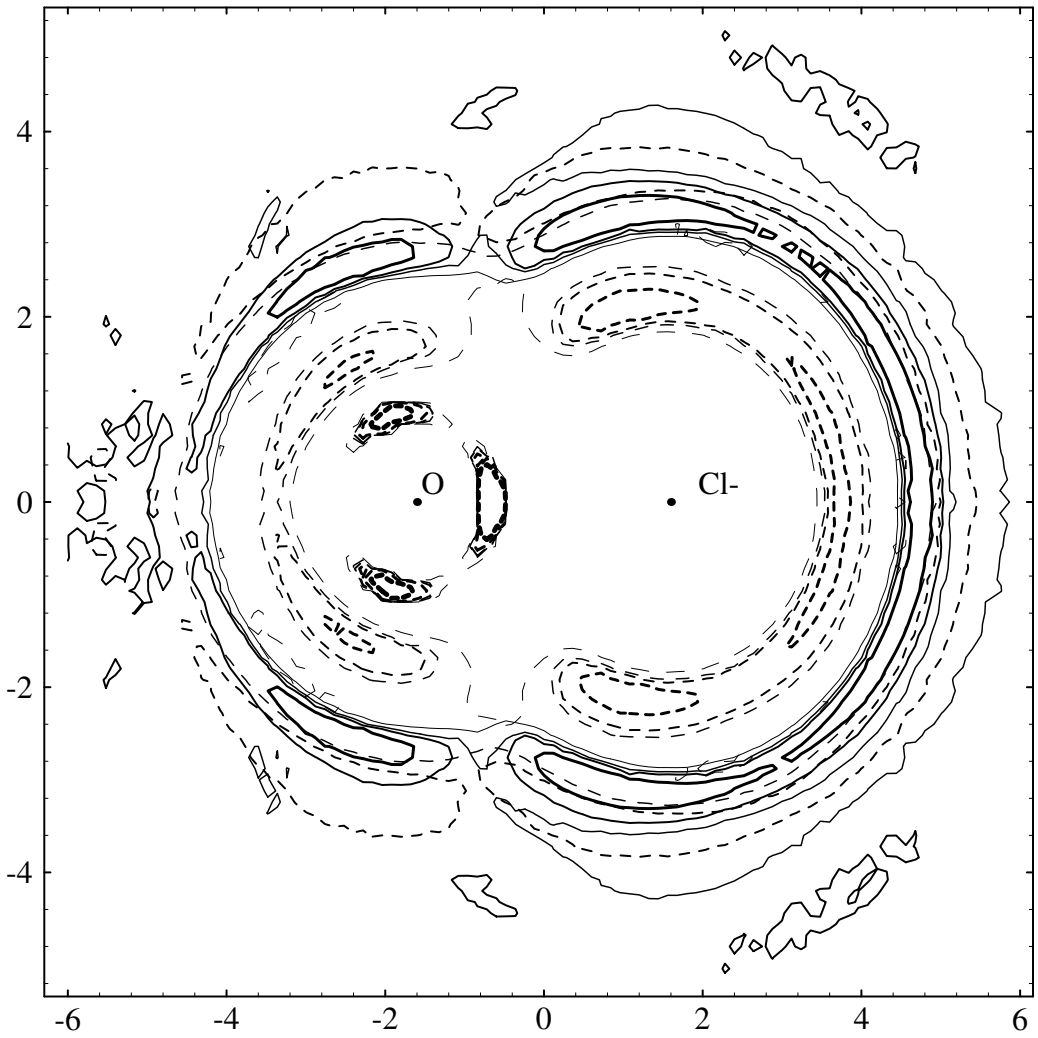
O
Cl-
4
2
0
-2
-4
-6
-4
-2
0
2
4
6

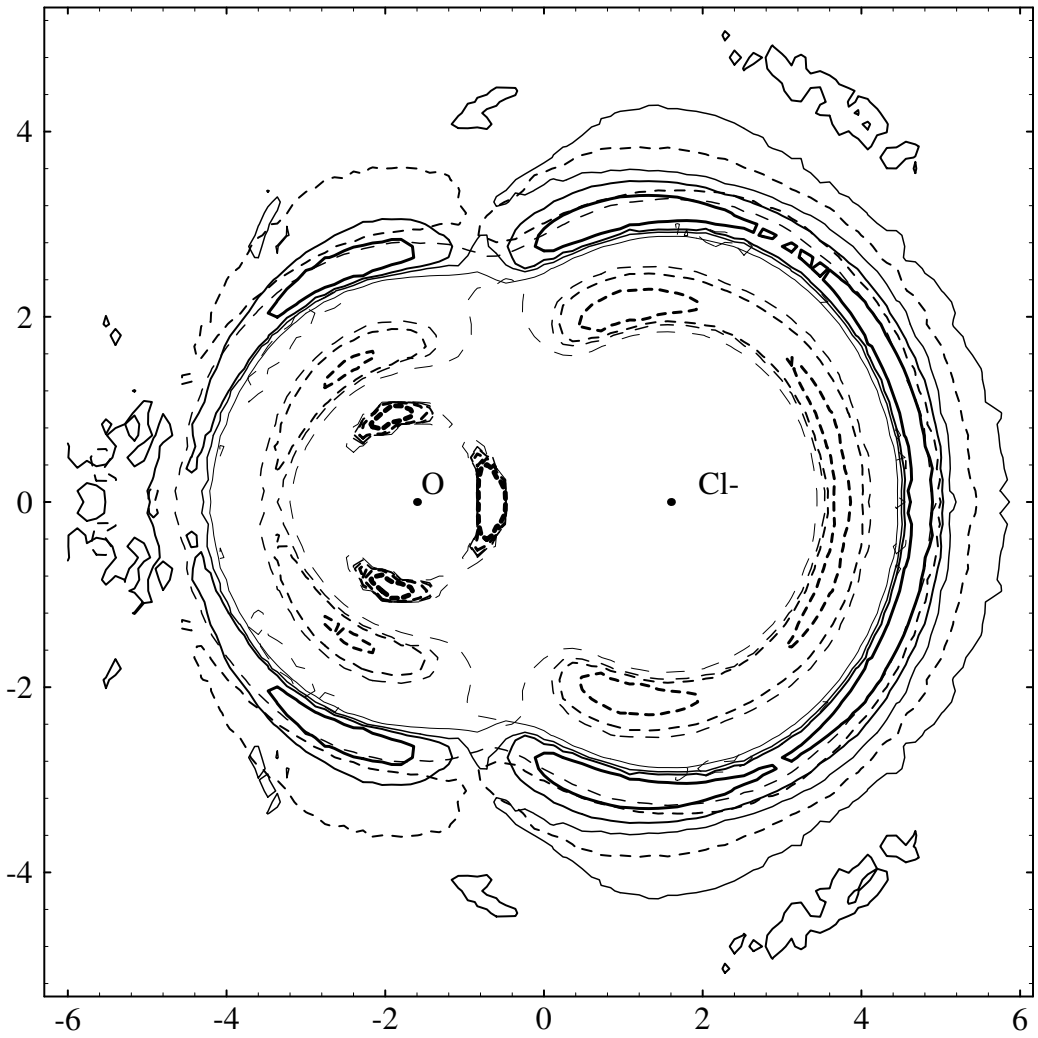
O
Cl-
4
2
0
-2
-4
-6
-4
-2
0
2
4
6

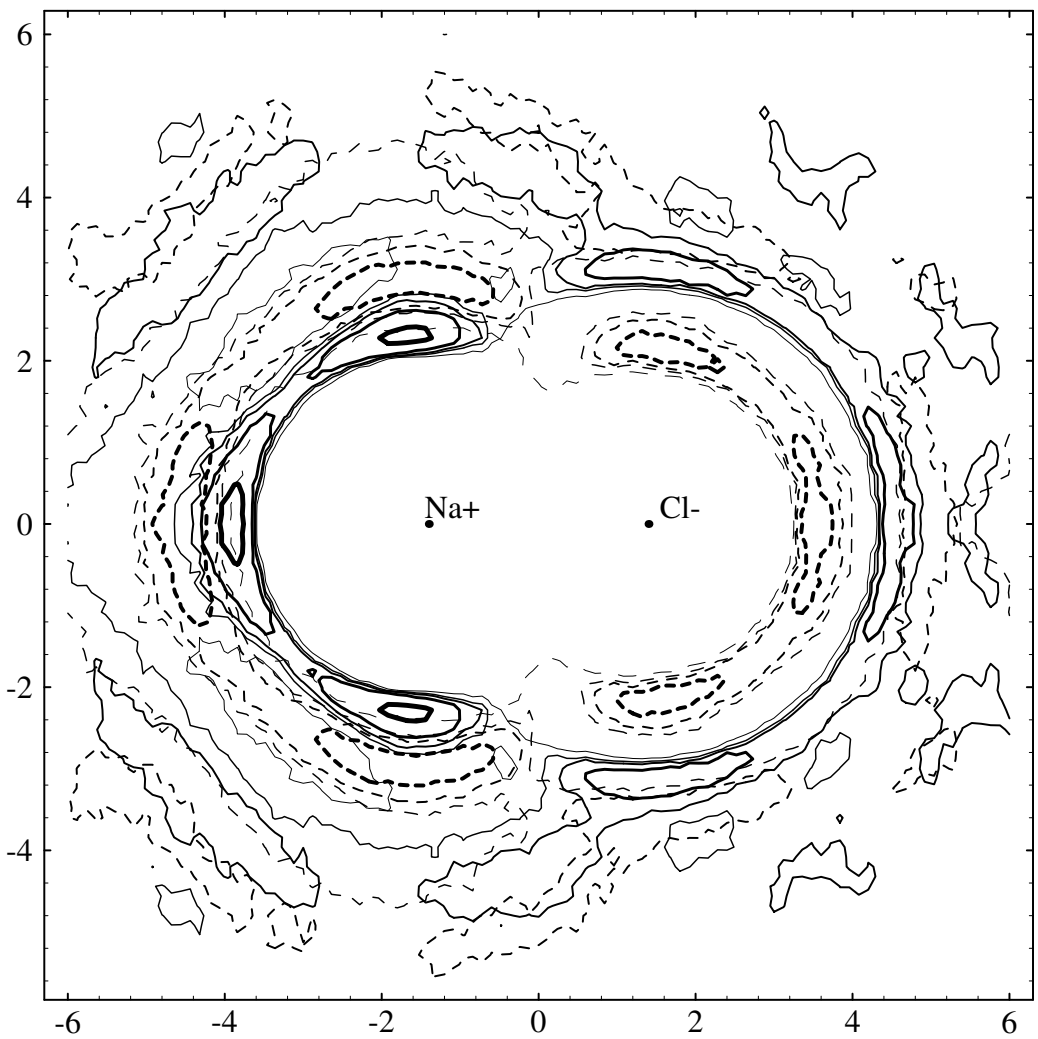
6
4
2
0
-2
-4
-6
-4
-2
0
2
4
6
Na+
Cl-

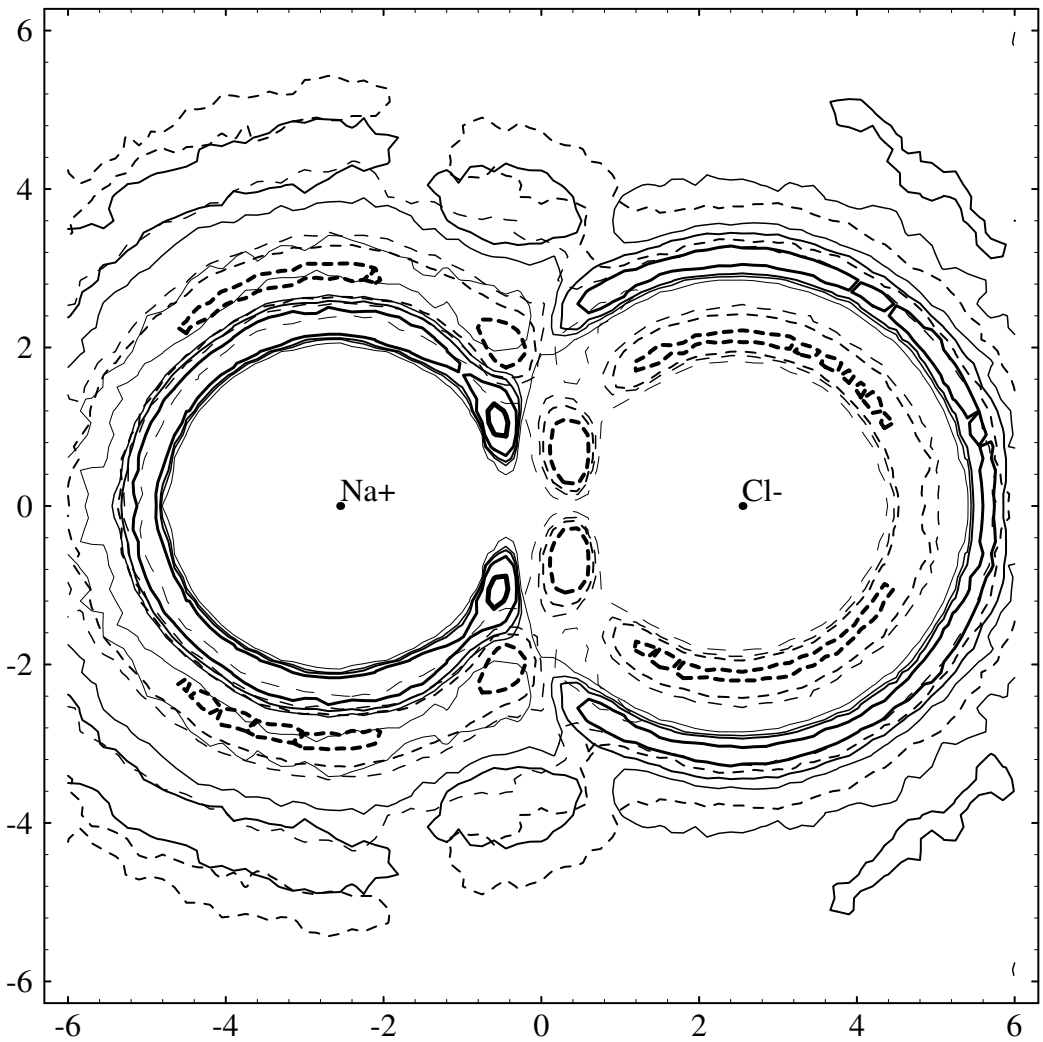
Na+
Cl-
6
4
2
0
-2
-4
-6
-6
-4
-2
0
2
4
6

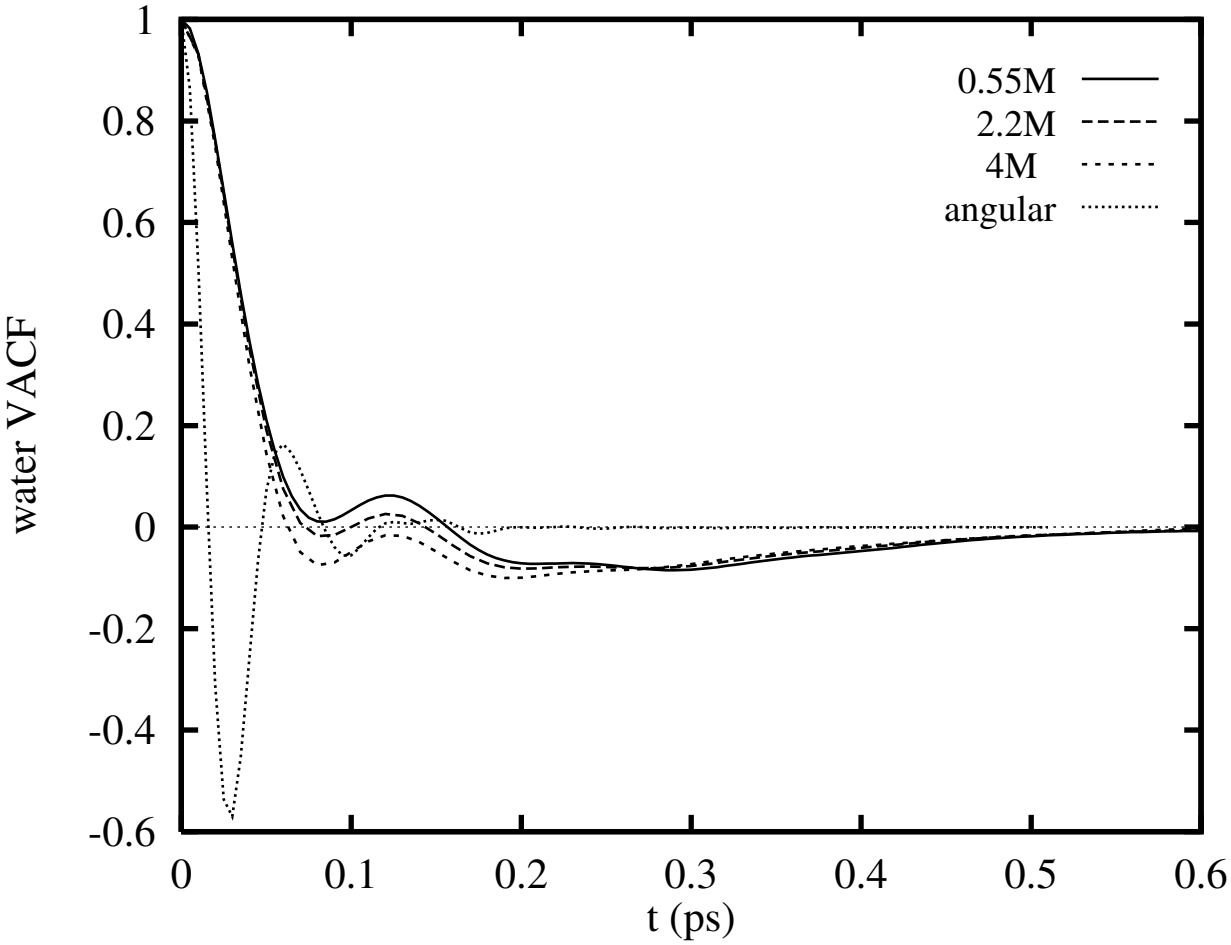
1
0.8
0.6
0.4
0.2
0
-0.2
-0.4
-0.6
0
0.1
0.2
0.3
0.4
0.5
0.6
water VACF
t (ps)
0.55M
2.2M
4M
angular

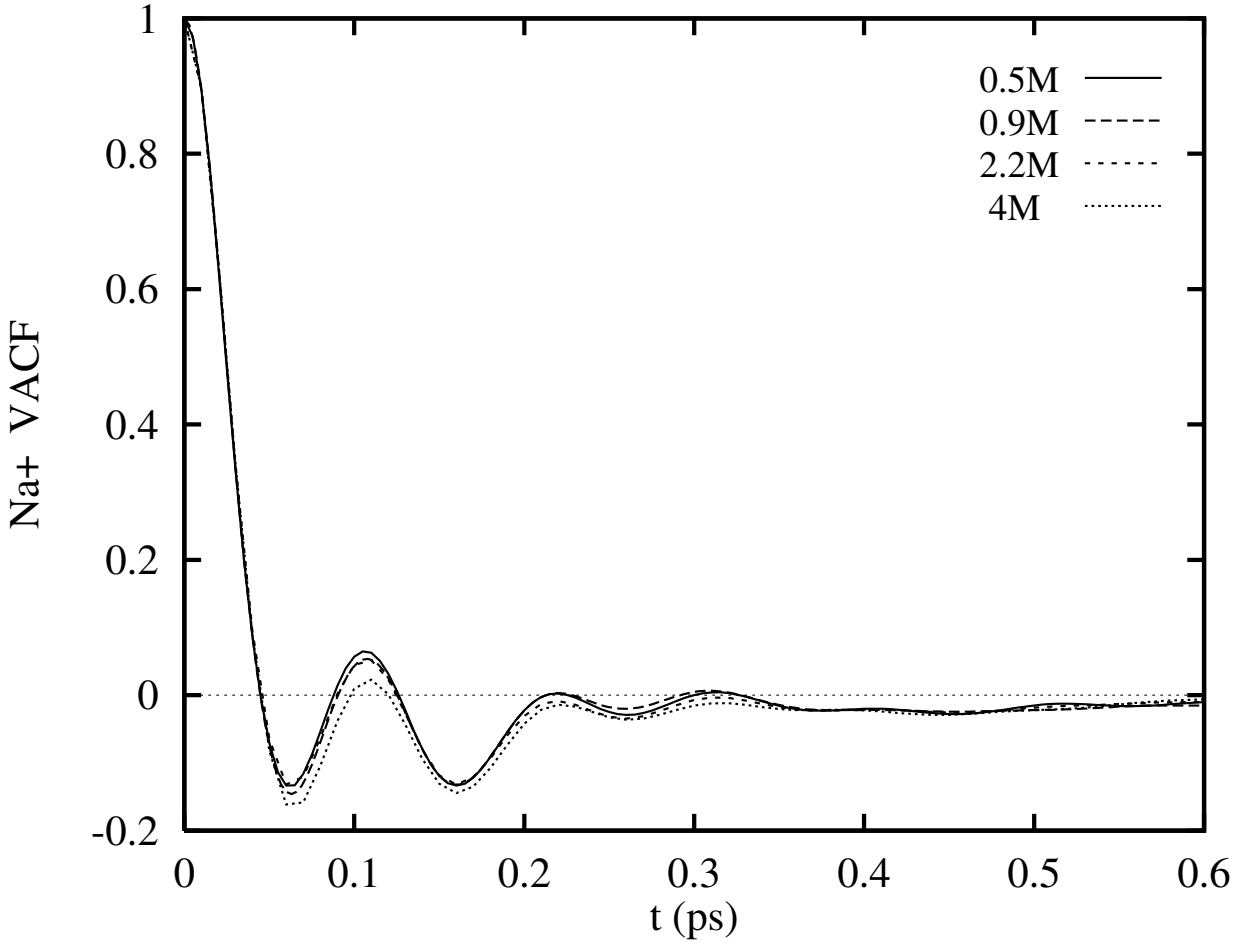
1
0.8
0.6
0.4
0.2
0
-0.2
0
0.1
0.2
0.3
0.4
0.5
0.6
Na+ VACF
t (ps)
0.5M
0.9M
2.2M
4M

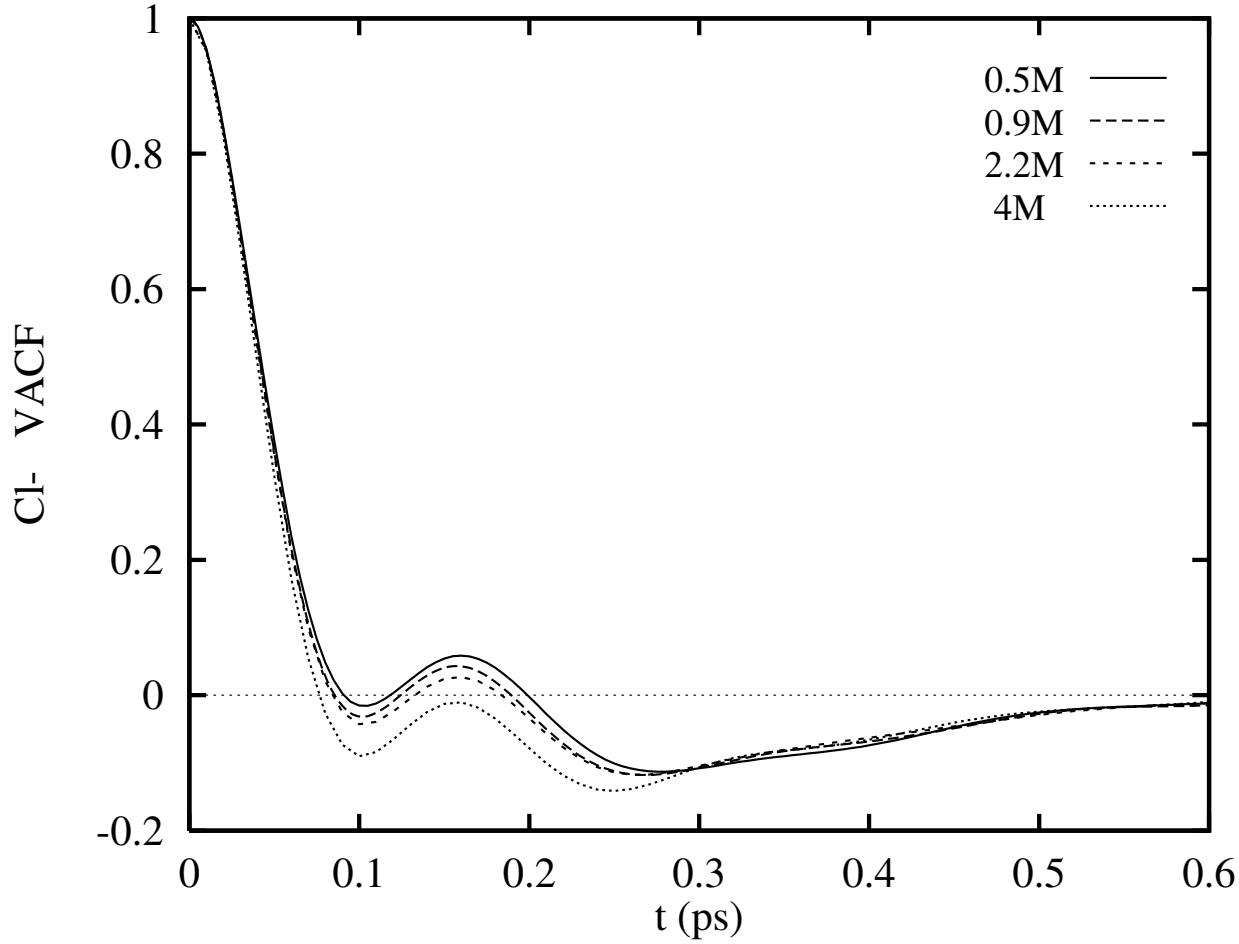
1
0.8
0.6
0.4
0.2
0
-0.2
0
0.1
0.2
0.3
0.4
0.5
0.6
Cl- VACF
t (ps)
0.5M
0.9M
2.2M
4M

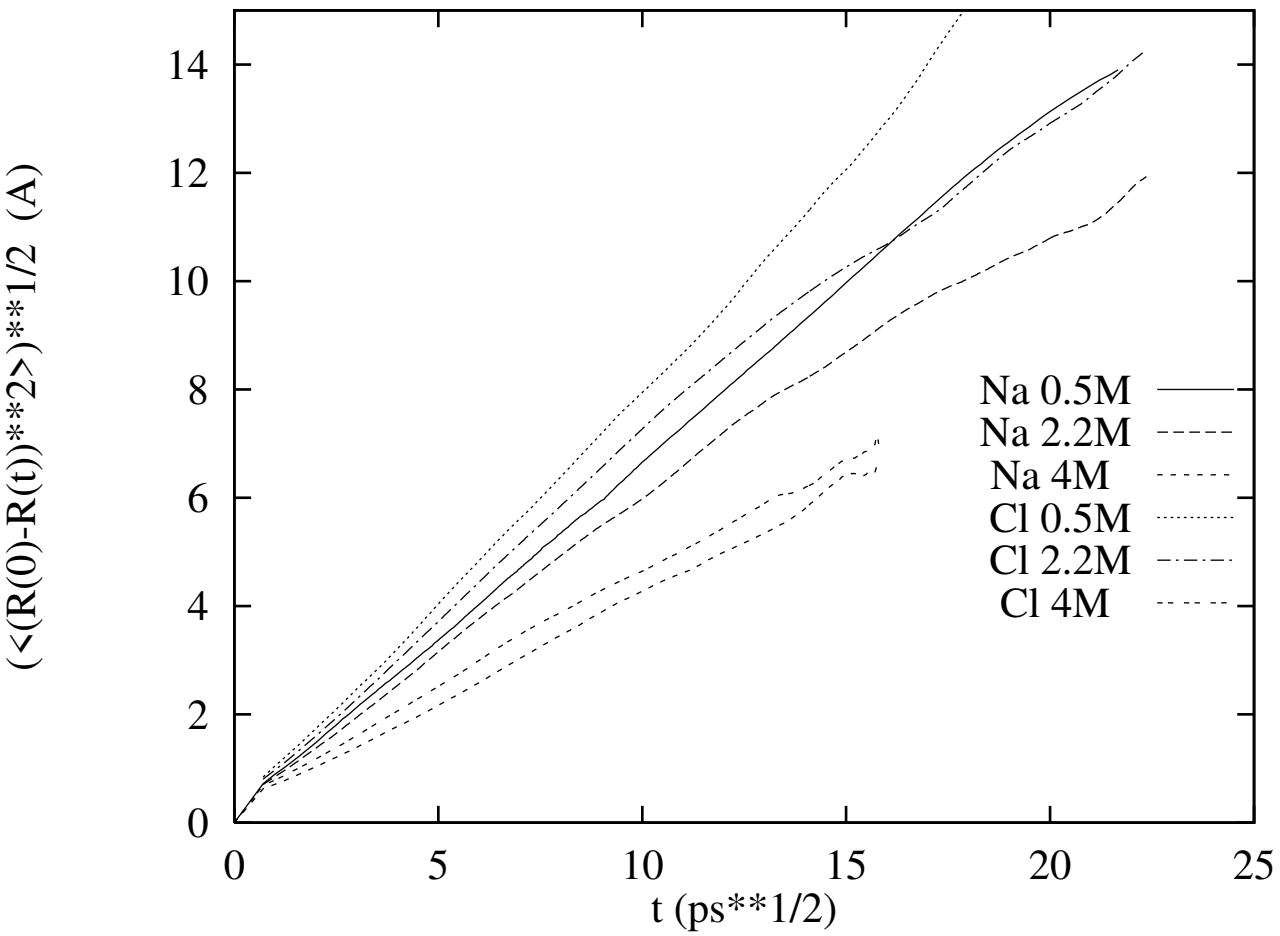
(<(R(0)-R(t))**2>)**1/2 (A)
t (ps**1/2)
0
2
4
6
8
10
12
14
0
5
10
15
20
25
Na 0.5M
Na 2.2M
Na 4M
Cl 0.5M
Cl 2.2M
Cl 4M

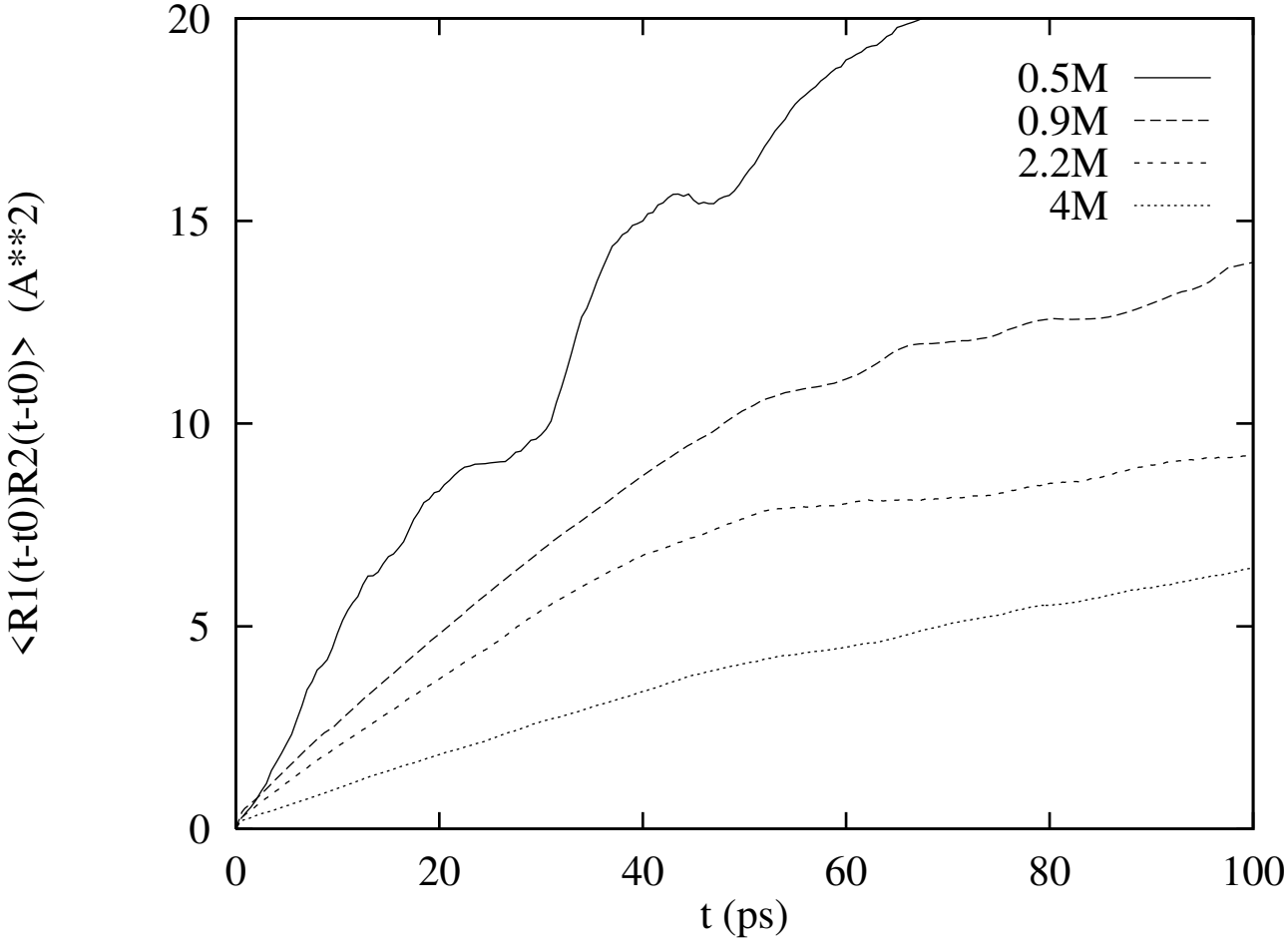
20
15
10
5
0
0
20
40
60
80
100
t (ps)
<R1(t-t0)R2(t-t0)> (A**2)
0.5M
0.9M
2.2M
4M

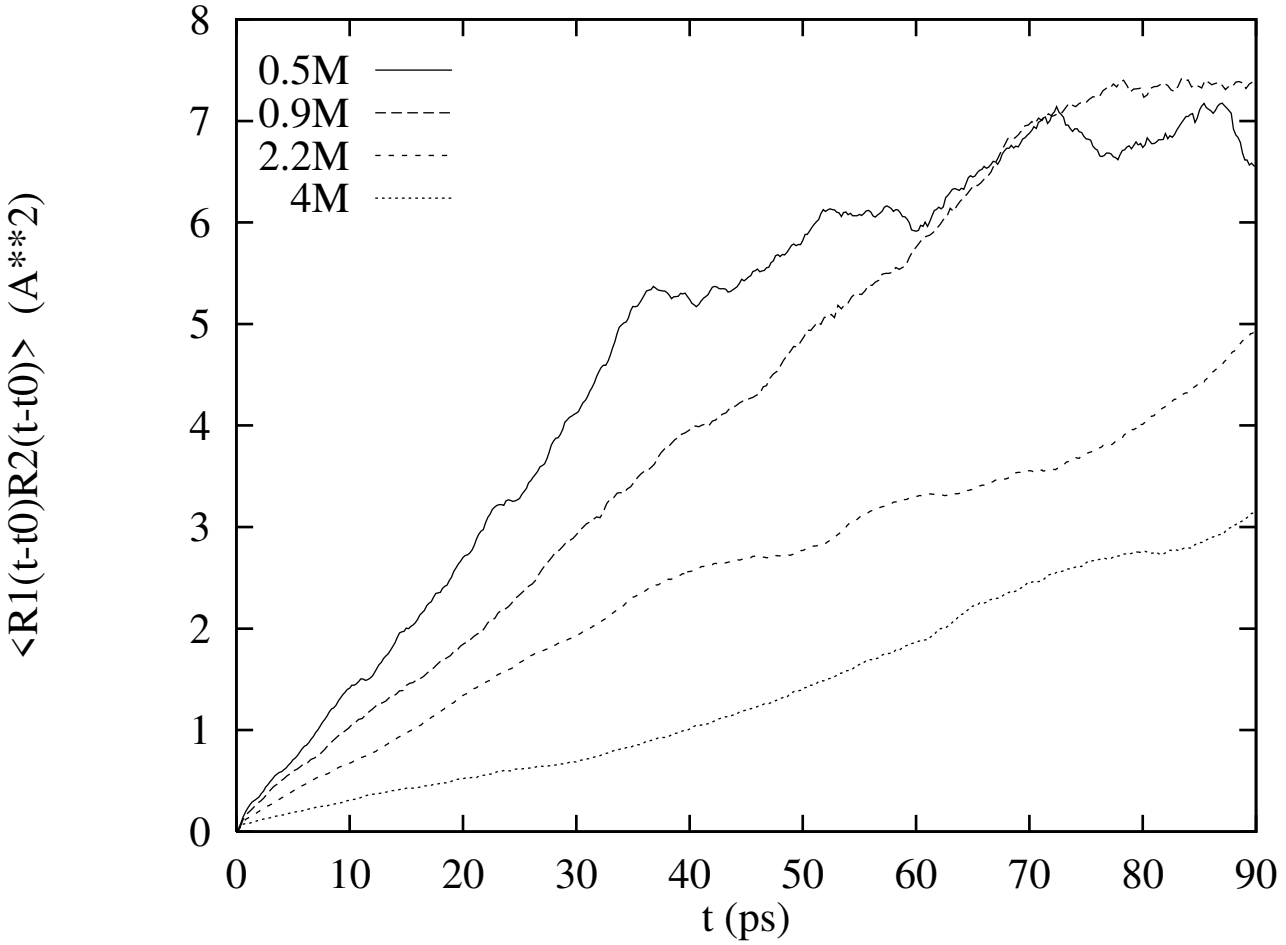
0.5M
0.9M
2.2M
4M
<R1(t-t0)R2(t-t0)> (A**2)
t (ps)
0
1
2
3
4
5
6
7
8
0
10
20
30
40
50
60
70
80
90

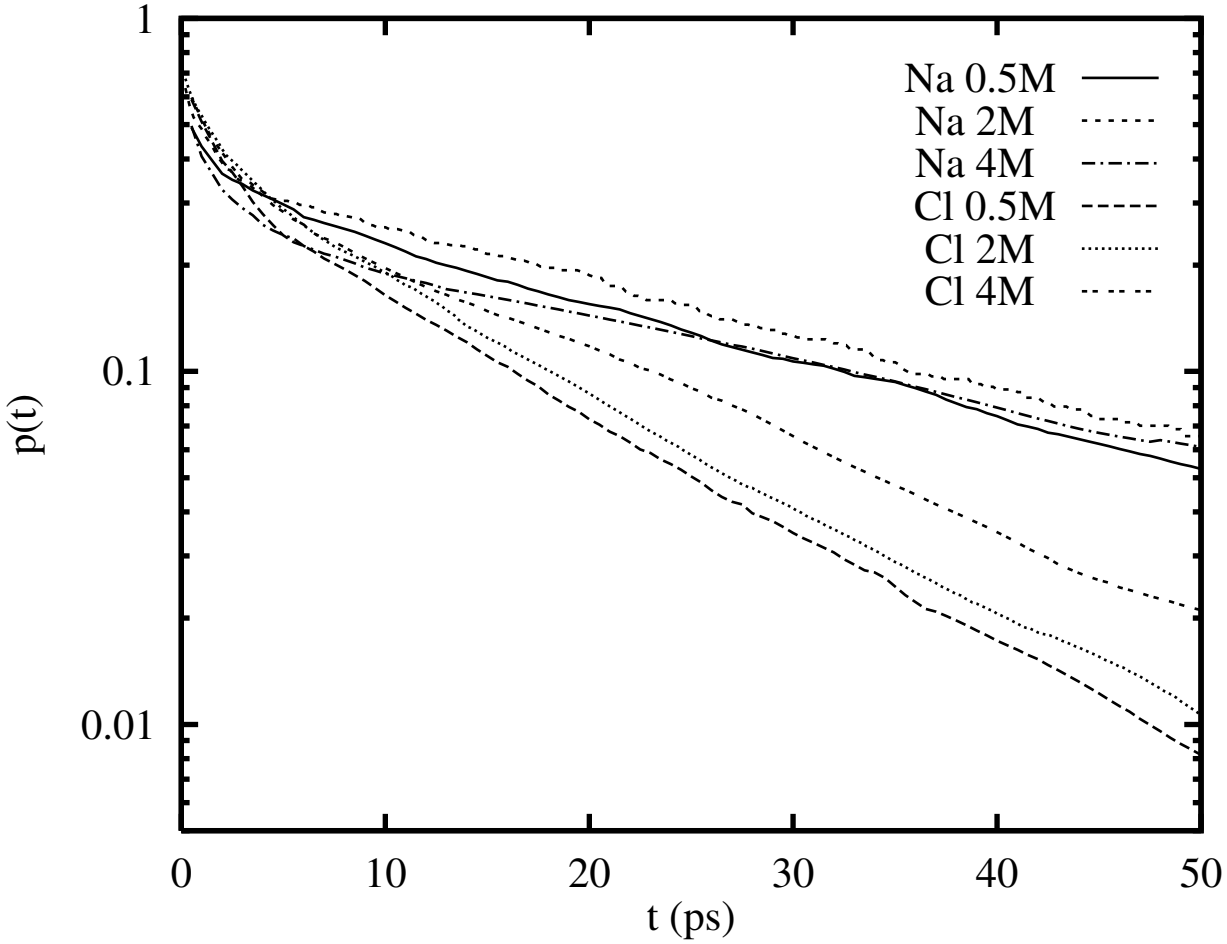
1
0.1
0.01
p(t)
0
10
20
30
40
50
t (ps)
Na 0.5M
Na 2M
Na 4M
Cl 0.5M
Cl 2M
Cl 4M

Offending Command = restore
Error = nametype : invalidrestore

Stack =
--nostringval--
--nostringval--